



Published in final edited form as:

*J Hepatol.* 2019 March ; 70(3): 458–469. doi:10.1016/j.jhep.2018.10.015.

## Impaired endothelial autophagy promotes liver fibrosis by aggravating the oxidative stress response during acute liver injury

Maria Ruart<sup>1,†</sup>, Laia Chavarria<sup>1,†</sup>, Genís Campreciós<sup>1,2</sup>, Nuria Suárez-Herrera<sup>1</sup>, Carla Montironi<sup>3</sup>, Sergi Guixé-Muntet<sup>4</sup>, Jaume Bosch<sup>1,2,4</sup>, Scott L. Friedman<sup>5</sup>, Juan Carlos Garcia-Pagán<sup>1,2</sup>, Virginia Hernández-Gea<sup>1,2,\*</sup>

<sup>1</sup>Barcelona Hepatic Hemodynamic Laboratory, Liver Unit, Hospital Clínic-Institut d'Investigacions Biomèdiques August Pi i Sunyer, University of Barcelona, Spain; <sup>2</sup>Centro de investigación Biomédica Red de enfermedades hepáticas y digestivas, Spain; <sup>3</sup>Pathology Department, Liver Cancer Translational Research Laboratory, BCLC Group, IDIBAPS, Liver Unit, Hospital Clínic, Spain; <sup>4</sup>Swiss Liver Centre, inselspital, Bern University, CH, Switzerland; <sup>5</sup>Division of Liver Diseases, Department of Medicine, Icahn School of Medicine at Mount Sinai, New York, United States

### Abstract

**Background & Aims:** Endothelial dysfunction plays an essential role in liver injury, yet the phenotypic regulation of liver sinusoidal endothelial cells (LSECs) remains unknown. Autophagy is an endogenous protective system whose loss could undermine LSEC integrity and phenotype. The aim of our study was to investigate the role of autophagy in the regulation of endothelial dysfunction and the impact of its manipulation during liver injury.

**Methods:** We analyzed primary isolated LSECs from *Atg7*<sup>control</sup> and *Atg7*<sup>endo</sup> mice as well as rats after CCl<sub>4</sub> induced liver injury. Liver tissue and primary isolated stellate cells were used to analyze liver fibrosis. Autophagy flux, microvascular function, nitric oxide bioavailability, cellular superoxide content and the antioxidant response were evaluated in endothelial cells.

**Results:** Autophagy maintains LSEC homeostasis and is rapidly upregulated during capillarization *in vitro* and *in vivo*. Pharmacological and genetic downregulation of endothelial autophagy increases oxidative stress *in vitro*. During liver injury *in vivo*, the selective loss of

\* Corresponding author. Address: Barcelona Hepatic Hemodynamic Laboratory, Liver Unit, Hospital Clínic, Villarroel 170, Barcelona 08036, Spain. Tel.: +34 932275400, (2209); Fax: +34 932279856. vihernandez@clinic.cat (V. Hernández-Gea).

<sup>†</sup>Both authors contributed equally to this work.

#### Authors' contributions

M.R. & L.C. designed the research, conceived ideas, performed experiments, and wrote the manuscript. G.C. and N.S.H. performed experiments and analyzed data. C.M. performed the histological analysis. S.G-M, J.B., S.L.F. and J.C.G.-P. critically revised the manuscript. V.H-G. designed the research, conceived ideas, wrote the manuscript, obtained funding and directed the study. All authors edited and reviewed the final manuscript.

#### Conflict of interest

The authors declare no conflicts of interest that pertain to this work.

Please refer to the accompanying ICMJE disclosure forms for further details.

#### Supplementary data

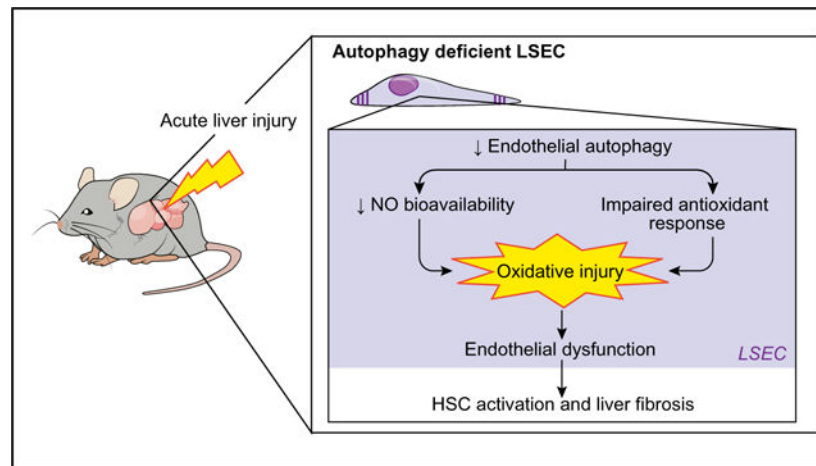
Supplementary data to this article can be found online at <https://doi.org/10.1016/j.jhep.2018.10.015>.

endothelial autophagy leads to cellular dysfunction and reduced intrahepatic nitric oxide. The loss of autophagy also impairs LSECs ability to handle oxidative stress and aggravates fibrosis.

**Conclusions:** Autophagy contributes to maintaining endothelial phenotype and protecting LSECs from oxidative stress during early phases of liver disease. Selectively potentiating autophagy in LSECs during early stages of liver disease may be an attractive approach to modify the disease course and prevent fibrosis progression.

**Lay summary:** Liver endothelial cells are the first liver cell type affected after any kind of liver injury. The loss of their unique phenotype during injury amplifies liver damage by orchestrating the response of the liver microenvironment. Autophagy is a mechanism involved in the regulation of this initial response and its manipulation can modify the progression of liver damage.

### Graphical abstract



### Keywords

Autophagy; Endothelial dysfunction; Liver fibrosis; Oxidative stress; LSEC; Nrf2; Endothelial cell; Atg7; Nitric oxide; eNOS

### Introduction

Chronic liver injury from any source leads to progressive fibrosis, yet treatments are elusive. A better understanding of the early changes that disrupt cellular homeostasis, and initiate and perpetuate fibrogenesis following liver injury is needed. Liver sinusoidal endothelial cells (LSECs) constitute the liver's first barrier of defense because of their unique position lining the sinusoidal lumen. They are also the initial liver cell type to sense injury. Maintenance of the LSEC phenotype associated with cellular pores, or fenestrae, is critical to maintaining homeostasis in the whole liver parenchyma. Following hepatic damage, sinusoidal endothelial dysfunction may arise and it is characterized by the loss of both fenestrae (capillarization) and of its anti-fibrotic, anti-thrombotic and anti-vasodilatory properties, which are essential for the maintenance of liver integrity.<sup>1</sup> LSEC injury also plays an essential role in initiation and progression of liver injury. Indeed, signals derived from the sinusoidal endothelium during liver damage determine the outcome of pro-regenerative vs.

pro-fibrotic processes.<sup>2,3</sup> Despite its primary role in maladaptive healing and liver fibro-sis, <sup>4,5</sup> the phenotypic regulation of endothelial dysfunction is not fully understood.

Autophagy is a major intracellular recycling system that maintains cellular homeostasis under basal conditions, and plays an integral role in regulating the cellular adaptive response during stress.<sup>6</sup> Although autophagy has been implicated in the regulation of other resident liver cells (hepato-cytes,<sup>7</sup> stellate cells<sup>8</sup> and macrophages<sup>9,10</sup>) and cardiovascular endothelial cell biology and physiopathology,<sup>11</sup> its role in regulating liver endothelial phenotype during acute liver injury remains largely unknown.

In the present study we hypothesized that endothelial autop-hagy is an endogenous protective system whose loss could undermine LSEC integrity and phenotype, ultimately leading to liver fibrosis. Therefore, the aim of our study was to investigate the role of autophagy in the regulation of endothelial dysfunction and the impact of its manipulation during liver injury.

## Materials and methods

### Animals

Animals were housed in polycarbonate cages and maintained in a temperature and light controlled facility under standard food and water *ad libitum*. All procedures were performed in accordance with Spanish legislation and approved by the Animal Research Committee of the University of Barcelona and were conducted in accordance with the European Community guide-lines for the protection of animals used for experimental and other scientific purposes (EEC Directive 86/609).

**Generation of endothelial—Cell-specific *Atg7* knockout mice** Previously described *Atg7<sup>Fllox/Fllox</sup>* mice on the C57BL/6 back-ground<sup>12</sup> were crossed with a line expressing Cre recombinase under the control of the VE-Cadherin promoter to generate *Atg7-VE-Cadherin-Cre (Atg7<sup>endo</sup>)* mice, a mouse model with a selective deficiency of the essential autophagy gene *Atg7* in endothelial cells.

**Induction of fibrosis in mice**—Carbon tetrachloride (CCl<sub>4</sub>) (Sigma) was used to induce mild acute liver injury. Mice received 3 intraperitoneal (i.p.) injections of 10% CCl<sub>4</sub> (diluted in olive oil) at a dose of 0.5 µl/g body weight<sup>13</sup> or vehicle (olive oil) every other day for 1 week.<sup>8</sup> Animals were sacrificed 48 h after the last dose under ketamine/midazolam anesthesia. At least 5 animals per group were used in isolation experiments and 6 to 12 animals per group in total tissue experiments making a total of 81 mice analyzed. All experiments were performed with mice between 10 and 14 weeks of age. We analyzed the effect of liver injury in male and female mice and the effect was similar in both genders, so all subsequent experiments were performed indistinctly in male and female mice.

**Induction of fibrosis in rats**—Hepatic injury was induced in 250–300 g male Sprague-Dawley (SD) rats (Charles River) by CCl<sub>4</sub> (50% CCl<sub>4</sub> diluted in olive oil at a dose of 1 µl/g of body weight) with 3 i.p. injections per week for 1, 4 or 6 weeks and compared with control rats injected with vehicle (olive oil).<sup>13</sup> A minimum of 3 animals per group were used

in isolation experiments accounting for a total of 36 rats. Animals were sacrificed 48 h after the last dose (CCl<sub>4</sub>) under ketamine/midazolam anesthesia.

### Cell lines and culture conditions

Unless otherwise specified, chemicals were purchased from Sigma-Aldrich (St. Louis, MO, USA). Culture media and supplements for cell culture were from Gibco-Invitrogen (Carlsbad, CA, USA) and plastic ware was from TPP (Trasadingen, Switzerland). Human umbilical vein endothelial cells (HUVEC, Lonza) were cultured on gelatin coating with M-199 (Gibco) medium supplemented with 20% FBS, 1% L-Glutamine, 1% penicillin/streptomycin (PS) and 1% endothelial cellgrowth supplement (ECGS). Mouse LSECs (TSECs) were kindly provided by Dr. V Shah<sup>14</sup> and cultured with endothelial cell medium (ECM, Scien-Cell) with 5% FBS, 1% PS and 1% ECGS. Rat and mouse LSECs as well as mouse hepatic stellate cells (HSCs) were isolated as previously described.<sup>15,16</sup> In brief, livers were perfused through the portal vein and digested with a collagenase solution. After mincing the liver, cells were filtered and centrifuged at 50xG to remove hepatocytes. Non-parenchymal cells were then separated by differential centrifugation using a Percoll gradient. Kupffer cells were eliminated by plastic pre-culture for 30 min. LSEC were plated in collagen coating dishes in RPMI-1640 medium with 10% FBS, 1% L-Glutamine, 1% PS, 1% Fungi-zona (Reactiva) and 1% ECGS. HSC cells were cultured in DMEM/F12 with 20% FBS, 1% PS and 1% Fungizona.

**ROS induction studies**—HUVECs and TSECs were seeded in 6-well plates and grown for 24 h before treatment with hydrogen peroxide (0.25 and 120  $\mu$ M, respectively) and collected after 72 h.

### Western blotting

Extracted proteins were analyzed by western blot. Antibodies used were: SQSTM1/p62 (Cell Signaling, 1/1000), LC3B [MAP1LC3B] (Cell Signaling, 1/1000), ATG7 (Cell signaling, 1/1000),  $\alpha$ SMA [ACTA2] (Sigma, 1/1000), PDGFRB (Santa Cruz, 1/500), total eNOS [NOS3] (BD Bioscience, 1/1000), eNOS phos-phorylated Ser1177 (Cell Signaling, 1/1000), HMOX1 (Enzo Life Sciences, 1/1000), NQO1 (Abcam, 1/1000). GAPDH (Santa Cruz, 1/1000) and  $\beta$ -actin [ACTB] (Sigma, 1/1000) served as house-keeping controls. Images were acquired with a LAS-3000 apparatus (Fujifilm, TDI, Alcobendas, Spain) and measurements made with the Multi Gauge software from Fujifilm following manufacturer's instructions. Protein ratios were normalized to housekeeping proteins ( $\beta$ -actin or GAPDH) and fold-change was calculated relative to control group.

**Autophagy flux:** As autophagy is a dynamic process influenced by the degradation activity of the cargo and recycling, autophagic flux was measured using the lysosomal inhibitor chloroquine (CQ) (20  $\mu$ M) for 2 h. Briefly, CQinhibits degradation of the cargo in the autophagosome leading to the accumulation of autophagic vacuoles that can be measured by quantifying the lipidated form of MAP1LC3B/LC3B (microtubule-associated protein 1 light chain 3 beta) (LC3B11) present in the autophagic vacuole membrane, using western blot.

### Quantitative real-time polymerase chain reaction

Total RNA was isolated by RNeasy Micro and Mini kit (Qiagen). First-strand cDNA was synthesized using the QuantiTect Reverse transcription kit (Qiagen) according to the manufacturer's instructions. Quantitative real-time PCR (qPCR) was performed using either TaqMan® Universal Master Mix or PowerUp™ SYBR® Green Master Mix (Applied Biosystems) with technical duplicates using an AB1 Prism® 7900 HT Cycler (Applied Biosystems). PCR cycle parameters were as follows: 95 °C for 10' followed by 40 cycles at 95 °C for 15'' and 60 °C for 1'. Results were obtained with the Sequence Detection System 3.2 software (Applied Biosystems) and further analyzed by the  $2^{-C_t}$  method. GAPDH or  $\beta$ -actin was used as a loading control. Results are shown as fold-change relative to the control group.

Primer specific sequences are listed in supplementary materials.

### Lentiviral Atg7 small interfering RNA construction

Lentiviral supernatants of small hairpin (sense-loop-antisense) RNAs against mouse *Atg7* (si*Atg7*) and its corresponding empty vector (VEC) were a kind gift from Dr. Czaja.<sup>8,17</sup> TSECs were transduced with lentivirus for 24 h followed by puromycin selection. Cultures were more than 90% GFP positive at the time experiments were performed.

### Histologic and immunohistochemical studies

Liver samples were formalin fixed, paraffin embedded and 4  $\mu$ m sections obtained. Hematoxylin and eosin (H&E) staining was performed for structural analysis. Sirius Red was used to determine collagen deposition; sections were stained with Sirius Red solution (saturated picric acid containing 0.1% Direct Red 80) to visualize collagen. The red stained area per total area was determined using AxioVision software and values are expressed as the mean of 10 fields at 20 $\times$  magnification obtained with a Zeiss Axiovert 135 microscope.

Immunohistochemical staining of aSMA, Von Willebrand factor (VWF) and desmin were performed with anti-aSMA (1/200, Abcam), anti-VWF (1/100, Dako) and anti-desmin (1/100, Dako). Bound antibodies were visualized with Dako REAL™ EnVision™ Detection System Peroxidase/DAB + kit, and slides were counterstained with hematoxylin. Fifteen images at 20  $\times$  magnifications were captured for immunohistochemical quantification with a Zeiss Axiovert 135 microscope and quantified with ImageJ software (NIH).

### Histological analysis

Histological analysis of the samples was performed on H&E stained slides by an expert pathologist. The inflammatory infiltrates in the liver parenchyma were evaluated in the portal, peri-central and lobular area using a score from 0 to 3 according to the following criteria: 0 = none; 1 = mild; 2 = moderate; 3 = severe. The regenerative aspect of hepatocytes was determined, considering the peculiarity of these cells' nucleus, by analyzing the presence of diploid hepatocytes and open chromatin, as well as the number of cells undergoing mitosis in the liver parenchyma. The assessment of necrosis was performed as follows: 1 = <5%; 2 = 5–29%; 3 = >30% of the analyzed parenchyma. Ballooning of hepatocytes was considered as 1 (mild) when it represented <4%, 2 (moderate) when it

represented between 5 and 15% of the hepatic cells and finally, 3 (marked) when ballooning was seen in >15% of the liver parenchyma.

### Hydroxyproline content

Hydroxyproline content was measured with Hydroxyproline Colorimetric Assay Kit (Biovision) following manufacturer's instructions.

Briefly, liver tissues were homogenized in H<sub>2</sub>Omilli-Q. HCl (12 M) was added to the homogenate and samples were incubated at 120 °C for 3 h. Kit reagents were added and absorbance at 560 nm was read in a plate reader and expressed as ng of hydroxyproline/mg liver.

### Electron microscopy

Livers were perfused through portal vein with a fixation solution containing 2.5% glutaraldehyde and 2% paraformaldehyde in 0.1 M sodium cacodylate, pH 7.4 and fixed overnight at 4 °C. Samples were washed 3 times with 0.1 M cacodylate buffer.

Transmission electron microscopy (TEM) was used to quantify the number of autophagosomes in LSECs. For TEM studies, fixed samples were then treated with 1% osmium tetroxide for 1 h, then dehydrated in acetone gradients and embedded in Spurr resin. Ultrathin sections (50 nm) were counterstained with uranyl acetate and lead citrate.<sup>18</sup> Samples were analyzed using a JEOLJ1010 electron microscope with an ORIUS camera (Gatan, Inc.; Roper Technologies, Inc.).

Scanning electron microscopy (SEM) was used to quantify liver sinusoidal fenestrae. Liver sections were fixed with 1% osmium in cacodylate buffer, dehydrated in ethanol, and dried with hexamethyldisilazane. Blocks were mounted onto stubs, and sputter coated with gold. Ten images per animal were acquired at a resolution of 15,000x using a JSM-6380 SEM (JEOL Ltd, Tokyo, Japan). Liver sinusoidal fenestrations were quantified using ImageJ software.<sup>18</sup> Porosity (percentage of LSEC surface occupied by fenestrae) was measured in SEM in liver tissue; in brief, total surface area and the open area of individual fenestrae were quantified.

### Measurement of the cellular superoxide content in liver tissue

*In situ* superoxide O<sub>2</sub><sup>-</sup> levels were assessed in HUVEC previously treated with either rapamycin or CQ, siAtg7TSECs and in fresh liver cryosections (10 μm) obtained from Atg7<sup>endo</sup> and control mice, with the oxidative fluorescent dye dihydroethidium (DHE; Molecular Probes Inc.) as described.<sup>19</sup> Six fields at 20x from each condition were randomly selected. Fluorescent images were obtained with an inverted microscope, Zeiss Axio-vert, and quantitative analysis was performed with ImageJ. In each experiment the same threshold was set for all images and integrated density (the product of Area and Mean Gray Value) was measured. For HUVECs and TSECs, the intensity was normalized to numbers of nuclei in each image.

### Cyclic guanosine monophosphate levels

Levels of cyclic guanosine monophosphate (cGMP) were measured as a marker of nitric oxide (NO) bioavailability in liver homogenates using an enzyme immunoassay following manufacturer instructions (Cayman Chemical Co., Ann Arbor, MI).<sup>19</sup> Briefly, equal amounts of liver tissue were dropped into 10 volumes of 5% trichloroacetic acid and homogenized at 4 °C. The precipitate was removed by centrifugation at 2000xG for 15 min at 4 °C. The supernatant was transferred to a clean test tube, washed with water-saturated diethyl ether 3 times and lyophilized. The dried extract was dissolved in assay buffer and cGMP levels were determined by enzyme immunoassay. Results were expressed as picomoles/g liver.

### Nitrotyrosine fluorohistochemistry

Quantitative tyrosine nitration detection was assessed as previously described.<sup>20,21</sup> Briefly, slides of liver sections were deparaffinized, hydrated, incubated with aqueous sodium dithionite solution (10 mM) for 10 min, washed with distilled water and then incubated overnight at 4 °C with an equimolar solution of AlCl<sub>3</sub> and salicylaldehyde (200 mM). Next morning, the aqueous solution was removed and sections were mounted in Fluoromount-G medium (Southern Biotech, Birmingham, AL). Negative and positive internal controls were included. Fluorescence images were obtained with a fluorescence microscope OLYMPUS BX51 and quantitative analysis of at least 6 images per sample was performed with ImageJ.

### Immunofluorescence

LSECs were seeded onto 12 mm micro coverglasses (Electron Microscopy Sciences). At different time-points (0 h, 24 h, 48 h), cells were fixed with 4% paraformaldehyde for 10min at room temperature, rinsed with PBS and permeabilized with 0.1% triton X-100 (Sigma) for 5 min. Thereafter, cells were blocked for 30 min with 1% BSA in PBS and consequently incubated with primary antibodies against LC3B (1:200, cell signaling) and Lamp2 (1:100, Santa Cruz) overnight at 4 °C.

Incubation with secondary antibodies conjugated with Alexa Fluor 488/555 (1:300, Invitrogen) was performed at room temperature for 1 h along with DAPI (3 ng/ml, Invitrogen). Preparations were then mounted using Fluoromount-G and dried overnight. Eight images per preparation and channel (visible; green, 488 nm; red, 555 nm) were obtained acquiring confocal z-stacks with a spectral confocal microscope (Leica TCS SPE). Images were then analyzed with the ImageJ software calculating the Pearson's coefficient per cell. The Pearson's correlation coefficient is a quantitative measurement that estimates the degree of overlap between fluorescence signals obtained in the 2 channels (green and red). The Pearson coefficients were averaged, and a standard error of the mean was calculated.<sup>22</sup>

### Statistical analysis

Statistical analysis was performed using SPSS 23.0 or GraphPad 5.01 for Windows. Groups were compared by ANOVA with *post hoc* tests when ANOVA analysis was significant (LSD and Tukey correction) or Student's t test when comparing 2 groups as adequate. All data are

reported as means  $\pm$  SEM. Differences were considered significant at a  $p$  value  $< 0.05$  with power of 80%.

## Results

### Autophagy is upregulated during LSEC capillarization *in vitro* and *in vivo*

After 24 h of growth on plastic in culture, isolated LSECs typically lose their fenestrated phenotype;<sup>4</sup> in the absence of growth factors, they become dysfunctional by 48 h and lose viability.<sup>23</sup> To link these changes to autophagic activity, freshly isolated LSECs from untreated SD rats were cultured up to 48 h on collagen-coated plastic. After 24 h in culture, LSECs expressed the previously reported typical transcriptional changes that accompany capillarization *in vitro*,<sup>4,24,25</sup> which include the downregulated expression of vascular endothelial growth factor receptor 2 (*Vegfr2 [Kdr]*) and upregulation of endothelin-1 (*Edn1*) mRNAs (Fig. 1A). These changes were accompanied by increased autophagic activity. As seen in Fig. 1B, primary LSECs cultured for 24 h demonstrated enhanced autophagic flux based on an increase of LC3BII levels in the presence of the autophagy inhibitor CQ (Fig. 1B) and colocalization of LC3B and LAMP2 (Fig. 1C). However, after longer periods of culture (48 h) when LSECs are completely dysfunctional, autophagy levels began declining (Fig. 1B, C).

Because *in vitro* experiments, even using freshly isolated LSECs, may not adequately represent the complexity of the LSEC defenestration process, we determined whether autophagic activity increases during endothelial dysfunction *in vivo* after liver injury. SD rats were treated with CCl<sub>4</sub> (i.p. injection every other day) at different time-points and the grade of liver fibrosis was assessed. Whereas 1-week of CCl<sub>4</sub> did not induce either endothelial dysfunction or autophagy (data not shown), after 4 weeks mild fibrosis was induced and after 6 weeks fibrosis was severe; thus *in vivo* studies were conducted at 4 and 6 weeks. Cells isolated from SD rats with CCl<sub>4</sub>-induced mild fibrosis (4 weeks) or severe fibrosis (6 weeks) developed an abnormal phenotype characterized by downregulation of *Vegfr2* and upregulation of *Edn1* mRNAs (Fig. 1D). LSECs from rats with mild fibrosis displayed an augmented autophagy flux that recapitulated their *in vitro* response, but was unable to further increase when fibrosis was more severe (6 weeks) (Fig. 1E, Fig. S1), implicating a role of endothelial autophagy during early phases of liver injury. Also, in agreement with this observation, when dysfunctional LSECs isolated from rats with CCl<sub>4</sub>-induced mild fibrosis were cultivated on plastic, they were unable to further upregulate autophagy levels (Fig. S2).

These data suggest that upregulation of endothelial autophagy may play a role in the adaptive response at early stages of liver injury, but it is overcome if the damage persists, and thus endothelial dysfunction arises.

### Endothelial autophagy maintains LSEC homeostasis

We then addressed the prospect that endothelial autophagy might regulate the phenotype of LSECs and orchestrate the early response to liver injury. To determine the role of endothelial autophagy during liver fibrosis *in vivo*, we generated a trans-genic mouse line in which

expression of the essential autophagy gene *Atg7* was specifically deleted in endothelial cells (*Atg7<sup>endo</sup>* mice) (Fig. 2). As previously described,<sup>12</sup> *Atg7<sup>flox/flox</sup>* mice<sup>26</sup> were crossed with mice carrying the Cre recombinase under the endothelial-specific promoter VE-cadherin (Jackson laboratory) (Fig. 2A). Primary LSECs were isolated from the *Atg7<sup>endo</sup>* mice and *Atg7* knockdown was confirmed by immunoblotting and qPCR (Fig. 2B,C). In agreement with previous studies,<sup>26</sup> LSECs isolated from *Atg7<sup>endo</sup>* mice displayed a downregulation of autophagy levels, indicated by a reduced number of autophagic vacuoles compared with their control littermates (*Atg7<sup>control</sup>*) when quantified by electron microscopy (Fig. S3), accumulation of p62 and decrease LC3BII/I ratio measured by western blot (Fig. 2C).

At baseline, mice with autophagy-defective LSEC (*Atg7<sup>endo</sup>*) displayed a normal liver architecture (Fig. 3A) without hepato-cyte injury (Fig. 3B) and did not show an obvious phenotype beyond a reduced body weight (Fig. 3C) when compared with their control littermates (*Atg7<sup>control</sup>*). However, following mild acute liver injury (1 week of CCl<sub>4</sub>)<sup>8</sup> *Atg7<sup>endo</sup>* mice developed amplified endothelial dysfunction (Fig. 4), demonstrated by the upregulation of mRNA levels of *Edn1* and downregulation of *Vegfr2* (Fig. 4A). Although these mRNAs have been proposed as surrogate markers of capillarization, it remained critical to evaluate the actual loss of fenestrae by SEM,<sup>27,28</sup> which is considered the gold standard technique for this purpose. SEM enables the assessment of large areas of the endothelial surface and measurement of size, frequency and porosity (the percent-age of LSEC membrane that is occupied by fenestra-tions).<sup>4,18,28,29</sup> SEM analysis confirmed a significant decrease in porosity and the number of fenestrae (Fig. 4B), further con-firming the greater level of endothelial dysfunction in the *Atg7<sup>endo</sup>* mice after mild acute liver injury. We also evaluated endothelial dysfunction in whole liver tissue by quantifying levels of the glycoprotein vWF, which were increased, consistent with a more dysfunctional phenotype (Fig. 4C).

Together, these data confirm that endothelial autophagy impairment provokes endothelial dysfunction, suggesting that as in other cells, autophagy may be an adaptive response to stress.

Loss of endothelial autophagy aggravates liver fibrosis with-out affecting liver inflammation

We next evaluated the role of autophagy in fibrosis after mild acute liver injury. In *Atg7<sup>endo</sup>* mice liver fibrosis was greatly amplified when compared with *Atg7<sup>control</sup>* mice (Fig. 5). Collagen accumulation evaluated by Sirius Red and hydroxyproline content was increased (Fig. 5A), together with the increased expression of the HSC activation marker  $\alpha$ SMA, as evaluated both by western blot analysis of primary isolated HSC and total liver immunohistochemistry (Fig. 5B,C). In contrast, there were no differences in the expression of desmin (Fig. 5C) or the proliferation marker PDGFRB (Fig. 5D), suggesting that the effect on fibrosis was due to activation of HSCs and not an increase in the total HSC number or their proliferation. Interestingly, *Atg7<sup>endo</sup>* mice had conserved regenerative capacity (Fig. 5E) and a similar degree of liver injury as *Atg7<sup>control</sup>* (Fig. 5E,F).

Interestingly, mild acute liver injury did not modify liver inflammation in our *Atg7<sup>endo</sup>* mice compared with *Atg7<sup>control</sup>* mice. Acute CCl<sub>4</sub>-induced injury induced mild pericentral inflammation similarly in the 2 groups of animals (Fig. 5G,H).

These results suggest that endothelial autophagy impairment under stress conditions (mild acute liver injury) aggravates liver fibrosis by directly activating HSCs.

### Loss of LSEC autophagy is associated with an insufficient antioxidant response

Reduction in endothelial NO bioavailability has been identified as one of the main governors of LSEC defenestration. Both a decrease in NO production and an increase in the reactive oxygen species O<sub>2</sub><sup>-</sup>, which reacts rapidly with NO to form peroxynitrite, reducing NO bioavailability. Moreover, oxidative stress plays a central role in the development and progression of liver fibrosis<sup>19</sup> by inducing oxidative injury and endothelial dysfunction.<sup>30,31</sup> Because autophagy has been identified as a major mechanism, which protects cells from oxidative stress in a wide range of cells,<sup>6,32-34</sup> we reasoned that autophagy might help to maintain LSEC phenotype providing an adequate redox balance in endothelial cells.

To mimic the effect of intracellular oxidative stress generation, we directly stimulated endothelial cells with exogenous H<sub>2</sub>O<sub>2</sub>. We used 2 different cell lines, human endothelial cells (HUVECs) and mouse LSECs (TSECs). H<sub>2</sub>O<sub>2</sub> provoked upregulation in autophagy in both cell lines (Fig. S4).

Therefore, we examined if pharmacological manipulation of endothelial autophagy modified oxidative stress. HUVECs were treated with the autophagy inhibitor CQ (Fig. 6A) or the autophagy inducer rapamycin (Fig. S5) and O<sub>2</sub><sup>-</sup> levels were measured by DHE; this data shows that inhibition of autophagy increases oxidative stress, which was attenuated when autophagy was upregulated. To establish a more specific link between autophagy and oxidant injury, TSECs were transduced with a lentiviral vector expressing small hairpin RNA to *Atg7* (si*Atg7* cells) or with an empty lentivirus control (VEC) (Fig. S6). As predicted, genetic deletion of *Atg7* amplified O<sub>2</sub><sup>-</sup> levels (Fig. 6B), further suggesting that endothelial autophagy maintains liver homeostasis at least in part by alleviating oxidative stress.

We next corroborated these data in vivo by evaluating oxidative stress levels in *Atg7<sup>endo</sup>* mice after mild acute liver injury. Intracellular O<sub>2</sub><sup>-</sup> production measured by DHE (Fig. 6C) and the content of hepatic nitrotyrosinate proteins, a fingerprint of peroxynitrite formation and a marker of NO scavenging by O<sub>2</sub><sup>-</sup> were markedly elevated (Fig. 6D) in whole liver tissue of the *Atg7<sup>endo</sup>* mice compared to *Atg7<sup>control</sup>* mice suggesting a decreased NO bioavailability. Indeed, cGMP a marker of intrahepatic NO availability, was significantly reduced in the *Atg7<sup>endo</sup>* mice compared to *Atg7<sup>control</sup>* mice (Fig. 6E).

Reduction in NO bioavailability may result from a decrease in endothelial NO production but also from impaired ROS removal.<sup>14-18</sup> Furthermore, recent data in vascular endothelial cells from kidney and the cardiovascular system have demonstrated that autophagy regulates eNOS production.<sup>19-22</sup> We therefore examined whether inhibition of autophagy impairs NO

production in our endothelial autophagy-deficient mice after CCl<sub>4</sub> induced liver injury. Decreased NO production due to reduced eNOS activity (measured by eNOS phosphorylation Ser1177/eNOS total ratio) was observed in the *Atg7<sup>endo</sup>* mice compared to *Atg7<sup>control</sup>* mice (Fig. 6F) suggesting that endothelial autophagy helps to cope with CCl<sub>4</sub>-induced oxidative stress by directly regulating intrahepatic NO bioavailability.

However, autophagy may control the antioxidant response in LSECs by additionally removing oxidative species. We evaluated the detoxifying response of LSECs after mild acute liver injury. We evaluated the classical antioxidant enzymes, superoxide dismutase (SOD), catalase (CAT) and glutathione peroxidase (GPx), in primary isolated LSECs from *Atg7<sup>endo</sup>* and *Atg7<sup>control</sup>* mice after acute CCl<sub>4</sub>-induced injury. As shown (Fig. 7A), a significant downregulation in these protective genes was observed. The antioxidant activity of these genes in whole liver tissue was also insufficient to alleviate the accumulation of oxidative species provoked by endothelial-specific autophagy impairment, reinforcing the importance of LSEC as the main scavenger cell type of the liver (Fig. S7).

The activity of the classical antioxidant genes can be bolstered by the so-called 'phase II detoxifying enzymes' regulated by the nuclear factor-erythroid 2-related factor 2 (Nrf2 [Nfe2l2]). Under oxidative stress, Nrf2 is phosphorylated and translocates into the nucleus, where it interacts with the antioxidant response element (ARE) within the promoters of genes encoding NADPH: quinone oxidoreductase 1 (*Nqo1*), heme oxygenase-1 (*Hmox1*), glutathione-S-transferase mu subunit (*Gstm*), glutamate-cysteine ligase catalytic (*Gclc*) and modulatory (*Gclm*) subunits and sulfiredoxin-1 (*Srxn1*).<sup>35,36</sup> Besides, Nrf2 can also be activated by the cytosolic protein p62 in conditions of autophagy deficiency. p62 degradation is impaired when autophagy is compromised and dissociates the redox-sensitive transcription complex Nrf2-Keap1, allowing Nrf2 to translocate to the nucleus and activate transcription of the ARE genes.<sup>37,38</sup> Indeed, as shown (Fig. 7B), the Nrf2-mediated antioxidant response in autophagy-deficient LSECs was upregulated, but was not sufficient to counteract the elevated oxidative stress, probably due, at least in part, to the shortage in NO. We also evaluated 2 of the main Nrf2-targets and further verify its upregulation at protein level (Fig. 7C), as an attempt to remove ROS in the *Atg7<sup>endo</sup>* mice. Remarkably, the Nrf2-mediated antioxidant response was unchanged in whole liver tissue, emphasizing the concept that impaired autophagy is the main trigger for Nrf2 activation and its activation may be limited to autophagy-deficient cells (Fig. S7).

All together these data support the concept that autophagy regulates LSEC response to oxidative stress by regulating both NO bioavailability and ROS removal.

## Discussion

Capillarization of sinusoids represents a change in LSEC phenotype characterized by the loss of fenestration, which induces HSC activation and liver fibrogenesis.<sup>1</sup> Although HSCs can be activated through other mechanisms during liver injury, signals coming from the endothelium determine and orchestrate the early liver response to a given injury.<sup>2,3</sup> Preventing endothelial dysfunction is an attractive therapeutic strategy that could interrupt

progression to liver fibrosis; however, the mechanisms controlling LSEC phenotypic changes are still not fully understood.

Our findings demonstrate that autophagic activity modulates LSEC capillarization. Loss of autophagy selectively in LSECs amplifies endothelial dysfunction and activates HSCs following mild acute liver injury. Basal autophagy in LSECs, as in other cells of the liver<sup>39</sup> is low, but it is rapidly upregulated as an adaptive response under conditions of cellular stress both *in vitro* and *in vivo*. In our *Atg7<sup>endo</sup>* mice, the moderate reduction of autophagy achieved in LSECs, may be sufficient to maintain adequate levels of endothelial autophagy under basal conditions to preserve a normal architecture. However, during early phases of injury, autophagy upregulation plays an important role in maintaining LSEC phenotype. Indeed, if the insult is

LSECs amplifies endothelial dysfunction and activates HSCs following mild acute liver injury. Basal autophagy in LSECs, as in other cells of the liver<sup>39</sup> is low, but it is rapidly upregulated as an adaptive response under conditions of cellular stress both *in vitro* and *in vivo*. In our *Atg7<sup>endo</sup>* mice, the moderate reduction of autophagy achieved in LSECs, may be sufficient to maintain adequate levels of endothelial autophagy under basal conditions to preserve a normal architecture. However, during early phases of injury, autophagy upregulation plays an important role in maintaining LSEC phenotype. Indeed, if the insult is either too intense or persists over time, autophagy induction is overcome leading to endothelial dysfunction and progressive fibrosis. In agreement with this concept, autophagy is rapidly upregulated in hepatocytes following alcohol injury in alcoholic liver disease, but over time there is a gradual loss of autophagy function,<sup>40</sup> supporting the idea that autophagy plays an essential role in early phases of the pathological process.

Remarkably, loss of LSEC autophagy provokes not only an exacerbation of endothelial dysfunction under conditions of cellular stress but also impacts the surrounding microenvironment by specifically modulating HSC activation. Indeed our transgenic animals did not have increased inflammation or prominent liver injury, supporting the concept that LSECs act as gatekeeper of HSC activation.<sup>28,41</sup>

NO has been previously identified as a master regulator of LSEC phenotype and contributes to maintaining redox balance. Because oxidant stress frequently accompanies liver injury and fibrogenesis and can induce autophagy,<sup>42</sup> we hypothesized that autophagy may preserve the LSEC phenotype at least in part by regulating NO, neutralizing ROS and maintaining cellular homeostasis. Indeed, exogenous ROS generation in endothelial cells was able to trigger autophagy. Moreover, disruption of endothelial autophagy, either pharmacologically or genetically, led to an aberrant antioxidant response and accumulation of ROS.

Our data also demonstrate that endothelial autophagy deficiency reduces intrahepatic NO bioavailability due to both decreased production and increased scavenging, which impairs the antioxidant response. In conditions of liver injury, where the demands of maintaining redox homeostasis are increased, autophagy-deficient LSECs are incapable of increasing NO levels to maintain their phenotype, ROS accumulates and endothelial dysfunction arises. LSECs are equipped with powerful antioxidant systems to remove ROS. The classical major

regulators of cellular redox balance antioxidant enzyme (CAT, SOD and GPx) could not be upregulated in LSECs from our *Atg7<sup>endo</sup>* mice during mild acute liver injury, leading to an inefficient adaptation to oxidative stress. This inability to cope with ROS and the loss of autophagy triggers Nrf2 activation and ARE upregulation to foster a more intense antioxidant response. The increase in p62 levels that accompanies autophagy impairment dissociates the redox-sensitive transcription complex Nrf2-Keap1 and leads to increased stabilization, translocation to the nucleus and activation of the transcription of the antioxidant genes *Nqol*, *Hmox1*, *Gstm*, *Gclc*, *Gclm* and *Srxn1*.<sup>38</sup> The upregulation of these genes in the *Atg7<sup>endo</sup>* mice reinforces the idea that autophagy regulates the antioxidant response in LSECs. Together, our data support the idea that autophagy-deficient LSECs are unable to neutralize the antioxidant stress that accompanies liver injury, in part due to an inefficient antioxidant response and inability to maintain adequate NO production. However, it remains to be elucidated whether upregulation of Nrf2 depends mainly on oxidant stress, autophagy deficiency or both.

Despite all the evidence supporting the association of oxidative stress and liver disease, how “antioxidant” compounds may regulate LSEC phenotype remains largely uncovered. Moreover, failure of antioxidant therapies in slowing fibrosis progression<sup>43–45</sup> in real clinical practice, favors the idea that interventions only removing ROS may not be enough. Indeed, we have shown that following acute CCl<sub>4</sub>-induced damage, LSEC de-differentiation due to autophagy dysfunction promoted decreased NO bioavailability, ROS accumulation and liver fibrogenesis, through HSC activation. Our data suggest that the inability of autophagy-deficient-LSECs to handle oxidative stress is responsible, at least in part, for promoting HSC activation; however, whether autophagy-mediated sinusoidal capillarization actively fosters HSC activation via release of specific paracrine mediators remains to be determined. Indeed, capillarized LSEC may contribute to HSC phenotypic and functional modulation not only by regulating NO production, but also by secreting other pro-fibrotic factors.<sup>2,3</sup>

Notwithstanding these functions, autophagy may also alleviate oxidative stress by other additional mechanisms such as removal of ROS-damaged organelles, such as the mitochondria and endoplasmic reticulum, as it has been demonstrated in other cell types, but it deserves detailed future specific studies in LSECs. Moreover, autophagy may also regulate other cellular pathways in LSECs besides NO and the antioxidant response. Indeed a previous study from our group demonstrated that autophagy upregulates the transcription factor KLF2 during ischemia-reperfusion injury and modulates endothelial survival.<sup>22</sup> Recently, autophagy has also been implicated in LSEC defenestration by controlling caveolin-1 expression.<sup>46</sup>

In conclusion, our data demonstrate that autophagy contributes to maintain cellular phenotype and protects LSECs from oxidative stress during early phases of liver injury, but may not be enough to revert damage in advanced stages of chronic liver injury. Endothelial autophagy dysregulation activates HSC and aggravates fibrosis during mild acute liver injury. Potentiation of autophagy selectively in LSECs during early stages of liver disease may be an attractive approach in order to prevent disease progression, thus modifying the natural course of chronic liver diseases.

## Supplementary Material

Refer to Web version on PubMed Central for supplementary material.

## Acknowledgments

The authors thank Biobank core facility of the Institut d'Investigacions Biomèdiques August Pi i Sunyer (IDIBAPS) for the technical help. We also thank Dr. Z Yue for the Atg7<sup>F/F</sup> mice, Dr. M. Czaja for the shAtg7 lentivirus and Dr. V Shah for the TSEC, Dr. A Diaz for the pathological support, J. Gracia-Sancho for experimental support, H Garcia-Caldero and M Monclús for their excellent technical assistance and R. Maeso for her experimental expertise. We also thank CERCA Programme/Generalitat de Catalunya.

Financial support

This work was sponsored by the Instituto de Salud Carlos III (ISCIII) PI14/00182, PI17/00298 and the European Union (Fondos FEDER, "Una manera de hacer Europa"). CIBERehd is funded by Instituto de Salud Carlos III. MR has a FPI grant from Ministerio de Economía y Competitividad related to SAF2013–44723-R & SAF2016–75767-R. LC has a Juan de la Cierva grant from the Instituto de Salud Carlos III.

## References

- [1]. DeLeve LD, Wang X, Guo Y. Sinusoidal endothelial cells prevent rat stellate cell activation and promote reversion to quiescence. *Hepatology* 2008;48:920–930. [PubMed: 18613151]
- [2]. Ding B-S et al. Divergent angiocrine signals from vascular niche balance liver regeneration and fibrosis. *Nature* 2014;505:97–102. [PubMed: 24256728]
- [3]. Ding B-S et al. Inductive angiocrine signals from sinusoidal endothelium are required for liver regeneration. *Nature* 2010;468:310–315. [PubMed: 21068842]
- [4]. Xie G et al. Hedgehog signalling regulates liver sinusoidal endothelial cell capillarisation. *Gut* 2013;62:299–309. [PubMed: 22362915]
- [5]. Pasarín M et al. Sinusoidal endothelial dysfunction precedes inflammation and fibrosis in a model of NAFLD. *PLoS ONE* 2012;7 e32785.
- [6]. Kroemer G, Marino G, Levine B. Autophagy and the integrated stress response. *Mol. Cell* 2010;40:280–293. [PubMed: 20965422]
- [7]. Singh R et al. Autophagy regulates lipid metabolism. *Nature* 2009;458:1131–1135. [PubMed: 19339967]
- [8]. Hernández-Gea V et al. Autophagy releases lipid that promotes fibrogenesis by activated hepatic stellate cells in mice and in human tissues. *Gastroenterology* 2012;142:938–946. [PubMed: 22240484]
- [9]. Lodder J et al. Macrophage autophagy protects against liver fibrosis in mice. *Autophagy* 2015;11:1280–1292. [PubMed: 26061908]
- [10]. Ilyas G et al. Macrophage autophagy limits acute toxic liver injury in mice through down regulation of interleukin-1  $\beta$ . *J Hepatol* 2016;64:118–127. [PubMed: 26325539]
- [11]. Lavandero S, Chiong M, Rothermel BA, Hill JA. Autophagy in cardiovascular biology. *J Clin Invest* 2015;125:55–64. [PubMed: 25654551]
- [12]. Torisu T et al. Autophagy regulates endothelial cell processing, maturation and secretion of von Willebrand factor. *Nat Med* 2013;19:1281–1287. [PubMed: 24056772]
- [13]. Ghiassi-Nejad Z et al. Reduced hepatic stellate cell expression of kruppel-like factor 6 tumor suppressor isoforms amplifies fibrosis during acute and chronic rodent liver injury. *Hepatology* 2013;57:786–796. [PubMed: 22961688]
- [14]. Huebert RC et al. Immortalized liver endothelial cells: a cell culture model for studies of motility and angiogenesis. *Lab Invest* 2010;90:1770–1781. [PubMed: 20644520]
- [15]. Gracia-Sancho J et al. Enhanced vasoconstrictor prostanoid production by sinusoidal endothelial cells increases portal perfusion pressure in cirrhotic rat livers. *J Hepatol* 2007;47:220–227. [PubMed: 17459512]

- [16]. Blomhoff R, Berg T. Isolation and cultivation of rat liver stellate cells. *Methods Enzymol* 1990;190:58–71. [PubMed: 1965004]
- [17]. Singh R et al. Autophagy regulates adipose mass and differentiation in mice. *J Clin Invest* 2009;119:3329–3339. [PubMed: 19855132]
- [18]. Le Couteur DG et al. Pseudocapillarization and associated energy limitation in the aged rat liver. *Hepatology* 2001;33:537–543. [PubMed: 11230732]
- [19]. Gracia-Sancho J et al. Increased oxidative stress in cirrhotic rat livers: a potential mechanism contributing to reduced nitric oxide bioavailability. *Hepatology* 2008;47:1248–1256. [PubMed: 18273863]
- [20]. Wisastra R et al. Antibody-free detection of protein tyrosine nitration in tissue sections. *ChemBioChem* 2011;12:2016–2020. [PubMed: 21748837]
- [21]. Hide D et al. A novel form of the human manganese superoxide dismutase protects rat and human livers undergoing ischaemia and reperfusion injury. *Clin Sci* 2014;127:527–537. [PubMed: 24754522]
- [22]. Guixé-Muntet S et al. Cross-talk between autophagy and KLF2 determines endothelial cell phenotype and microvascular function in acute liver injury. *J Hepatol* 2017;66:86–94. [PubMed: 27545498]
- [23]. DeLeve LD, Wang X, Hu L, McCuskey MK, McCuskey RS. Rat liver sinusoidal endothelial cell phenotype is maintained by paracrine and autocrine regulation. *Am J Physiol Gastrointest Liver Physiol* 2004;287: G757–G763. [PubMed: 15191879]
- [24]. Rockey DC, Chung JJ. Reduced nitric oxide production by endothelial cells in cirrhotic rat liver: endothelial dysfunction in portal hypertension. *Gastroenterology* 1998;114:344–351. [PubMed: 9453496]
- [25]. Géraud C et al. Liver sinusoidal endothelium: a microenvironment-dependent differentiation program in rat including the novel junctional protein liver endothelial differentiation-associated protein-1. *Hepatology* 2010;52:313–326.
- [26]. Komatsu M et al. Impairment of starvation-induced and constitutive autophagy in Atg7-deficient mice. *J Cell Biol* 2005;169:425–434. [PubMed: 15866887]
- [27]. Poisson J et al. Liver sinusoidal endothelial cells: physiology and role in liver diseases. *J Hepatol* 2017;66:212–227. [PubMed: 27423426]
- [28]. DeLeve LD. Liver sinusoidal endothelial cells in hepatic fibrosis. *Hepatology* 2015;61:1740–1746.
- [29]. Cogger VC, O'Reilly JN, Warren A, Le Couteur DG. A standardized method for the analysis of liver sinusoidal endothelial cells and their fenestrations by scanning electron microscopy. *J Vis Exp* 2015 , e2698.
- [30]. Guillaume M et al. Recombinant human manganese superoxide dismutase reduces liver fibrosis and portal pressure in CCl4-cirrhotic rats. *J Hepatol* 2013;58:240–246. [PubMed: 22989570]
- [31]. Di Pascoli M et al. Resveratrol improves intrahepatic endothelial dysfunction and reduces hepatic fibrosis and portal pressure in cirrhotic rats. *J Hepatol* 2013;58:904–910. [PubMed: 23262250]
- [32]. Scherz-Shouval R et al. Reactive oxygen species are essential for autophagy and specifically regulate the activity of Atg4. *EMBO J* 2007;26:1749–1760. [PubMed: 17347651]
- [33]. Mizushima N. Autophagy: process and function. *Genes Dev* 2007;21:2861–2873. [PubMed: 18006683]
- [34]. Filomeni G, De Zio D, Cecconi F. Oxidative stress and autophagy: the clash between damage and metabolic needs. *Cell Death Differ* 2015;22:377–388. [PubMed: 25257172]
- [35]. Hernández-Gea V et al. Endoplasmic reticulum stress induces fibrogenic activity in hepatic stellate cells through autophagy. *J Hepatol* 2013;59:98–104. [PubMed: 23485523]
- [36]. Marrone G et al. KLF2 exerts antifibrotic and vasoprotective effects in cirrhotic rat livers: behind the molecular mechanisms of statins. *Gut* 2015;64:1434–1443. [PubMed: 25500203]
- [37]. Puissant A, Fenouille N, Auberger P. When autophagy meets cancer through p62/SQSTM1. *Am J Cancer Res* 2012;2:397–413. [PubMed: 22860231]

- [38]. Komatsu M et al. The selective autophagy substrate p62 activates the stress responsive transcription factor Nrf2 through inactivation of Keap1. *Nat Cell Biol* 2010;12:213–223. [PubMed: 20173742]
- [39]. Cuervo AM, Knecht E, Terlecky SR, Dice JF. Activation of a selective pathway of lysosomal proteolysis in rat liver by prolonged starvation. *Am J Physiol* 1995;269:C12GG-C12G8.
- [40]. Ding W-X, Li M, Yin X-M. Selective taste of ethanol-induced autophagy for mitochondria and lipid droplets. *Autophagy* 2011;7:248–249.
- [41]. Xie G et al. Role of differentiation of liver sinusoidal endothelial cells in progression and regression of hepatic fibrosis in rats. *Gastroenterology* 2012;142:918–927.e6.
- [42]. Chen Y, Azad MB, Gibson SB. Superoxide is the major reactive oxygen species regulating autophagy. *Cell Death Differ* 2009;16:1G4G-1G52.
- [43]. Sanyal AJ et al. Pioglitazone, vitamin E, or placebo for nonalcoholic steatohepatitis. *N Engl J Med* 2010;362:1675–1685. [PubMed: 20427778]
- [44]. Harrison SA, Torgerson S, Hayashi P, Ward J, Schenker S. Vitamin E and vitamin C treatment improves fibrosis in patients with nonalcoholic steatohepatitis. *Am J Gastroenterol* 2003;98:2485–2490. [PubMed: 14638353]
- [45]. Ferenci P et al. Randomized controlled trial of silymarin treatment in patients with cirrhosis of the liver. *J Hepatol* 1989;9:105–113. [PubMed: 2671116]
- [46]. Luo X et al. Autophagic degradation of caveolin-1 promotes liver sinusoidal endothelial cells defenestration. *Cell Death Dis* 2018;9:576. [PubMed: 29760379]

**Highlights**

- Autophagy maintains liver endothelial cell homeostasis.
- Autophagy deficiency in LSEC increases oxidative stress.
- Autophagy regulates nitric oxide bioavailability and maintains LSEC phenotype.
- Impairment of endothelial autophagy enhances endothelial dysfunction and exacerbates fibrosis.

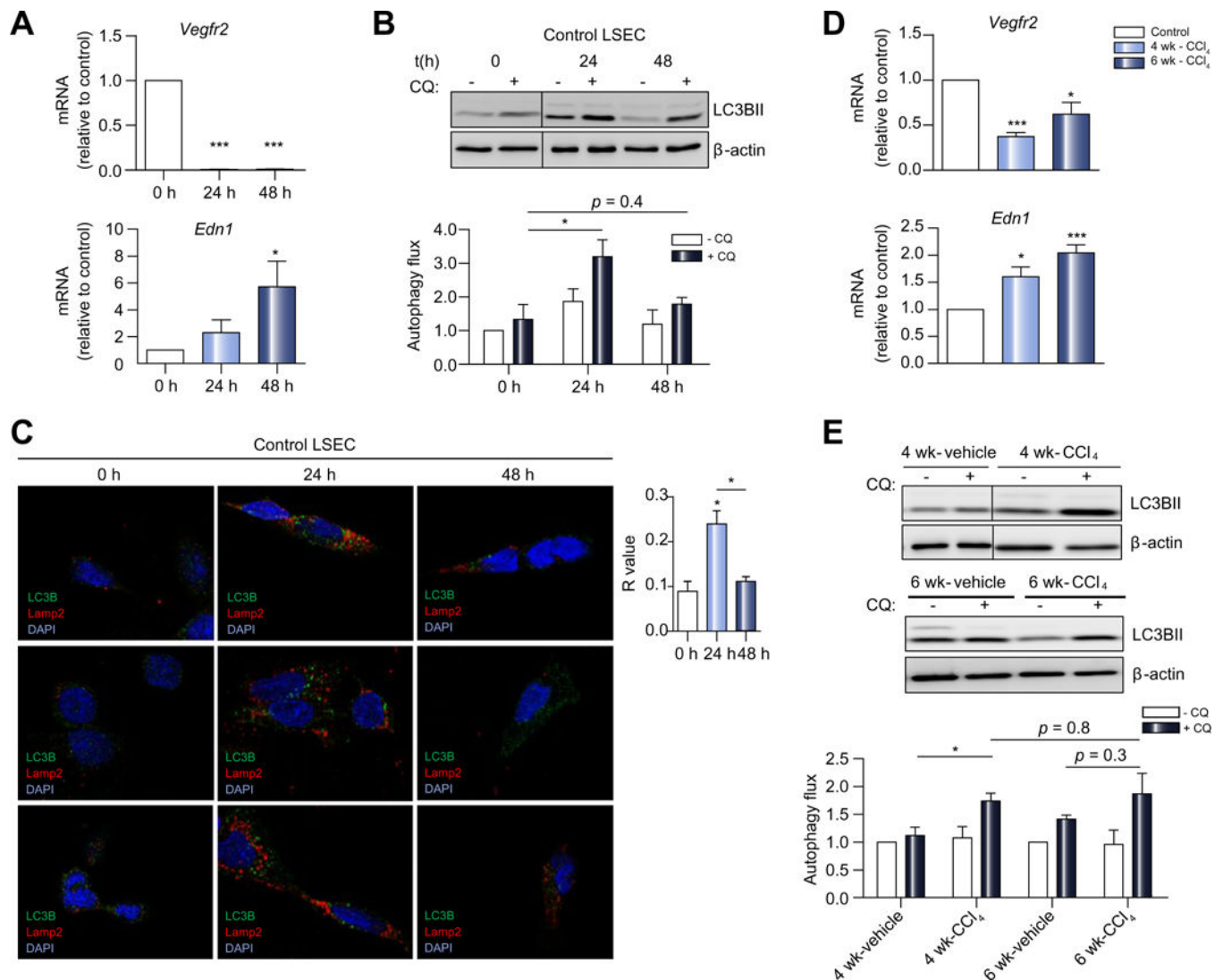


**Fig. 1. Autophagy is upregulated during *in vitro* and *in vivo* induced capillarization.**

Primary LSECs were isolated from untreated SD rats, directly plated ( $t = 0$  h) and grown on plastic tissue culture or onto coverglasses for 24 h ( $t = 24$  h) and 48 h ( $t = 48$  h). Cells were then fixed and processed for immunofluorescent microscopy. For autophagy flux assay by western blot cells were treated with CQ or vehicle during 2 h and collected thereafter. (A) mRNA changes (qPCR analysis) associated with endothelial dysfunction, showing a decrease in *Vegfr2* and an increase in *Edn1* and (B) LC3B11 immunoblotting with and without addition of CQ showing an increase in autophagy flux at 24 h that decreases at 48 h of culture. (C) Representative immunofluorescent images and quantification of autophagosomes (LC3B, green) with lysosomes (Lamp2, red) colocalization (R value) in LSECs confirming autophagy upregulation during capillarization. Primary LSECs isolated from rats treated with CCl<sub>4</sub> or vehicle for 4 and 6 weeks: (D) mRNA changes (qPCR analysis) associated with endothelial dysfunction, showing a decrease in *Vegfr2* and an increase in *Edn1* and (E) LC3B11 immunoblotting with and without addition of CQ showing autophagy flux displaying an increase at 4 weeks and incapability of further increase at 6

weeks. Data shows mean value  $\pm$  SEM of at least 3 experiments. mRNA and protein expressions are expressed as fold-change relative to control (\* $p$  0.05, \*\* $p$  0.01, \*\*\* $p$  0.001, Student's  $t$  test or ANOVA). CCl<sub>4</sub>, carbon tetrachloride; CQ chloroquine; LSEC, liver sinusoid endothelial cell; qPCR, quantitative real-time PCR; SD, Sprague-Dawley.

Author Manuscript

Author Manuscript

Author Manuscript

Author Manuscript

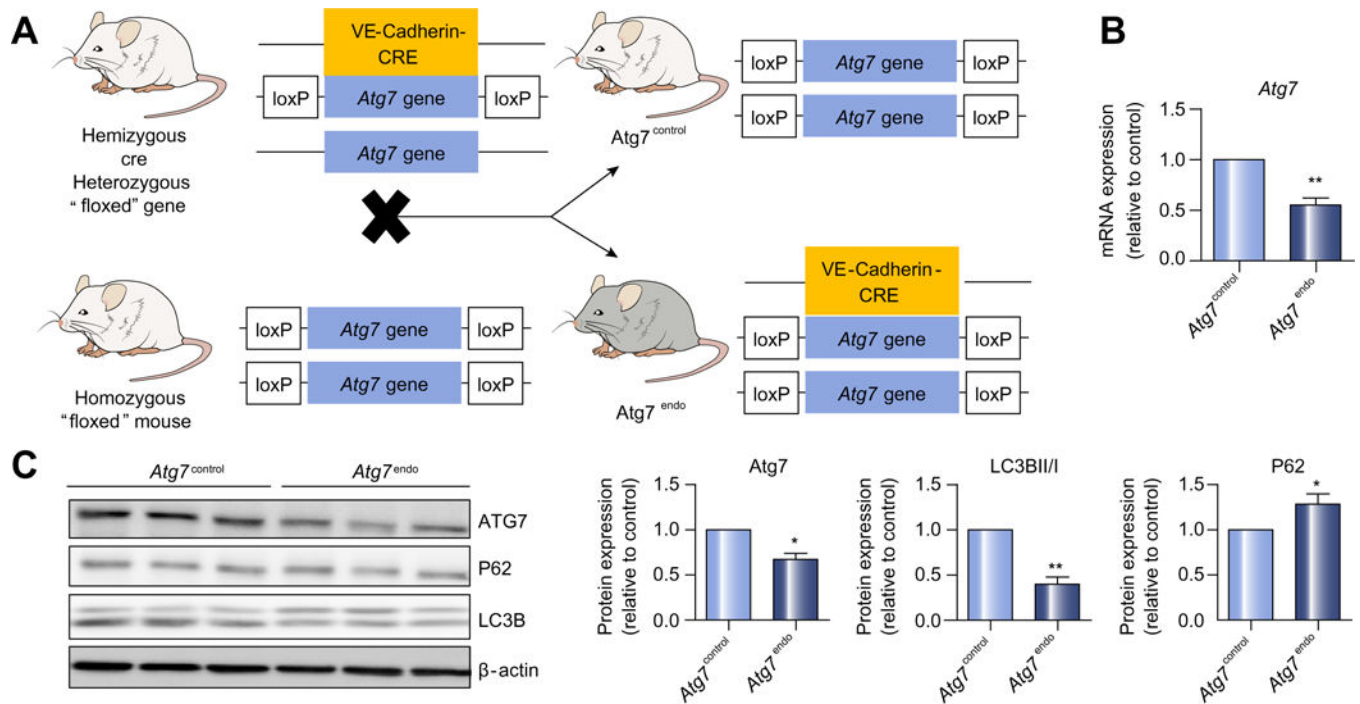


**Fig. 2. Generation of *Atg7*<sup>endo</sup> mice.**

(A) Schematic view of *Atg7*<sup>endo</sup> mice model generation. (B) mRNA changes (qPCR analysis) and (C) immunoblot of primary LSECs isolated from *Atg7*<sup>endo</sup> mice showing decreased expression of Atg7 and LC3B11/1 and increased of p62 levels. Data shows mean value  $\pm$  SEM of at least 3 experiments (\* $p$  0.05, \*\* $p$  0.01, \*\*\* $p$  0.001, Student's  $t$  test). LSEC, liver sinusoid endothelial cell; qPCR, quantitative real-time PCR. (This figure appears in colour on the web.)

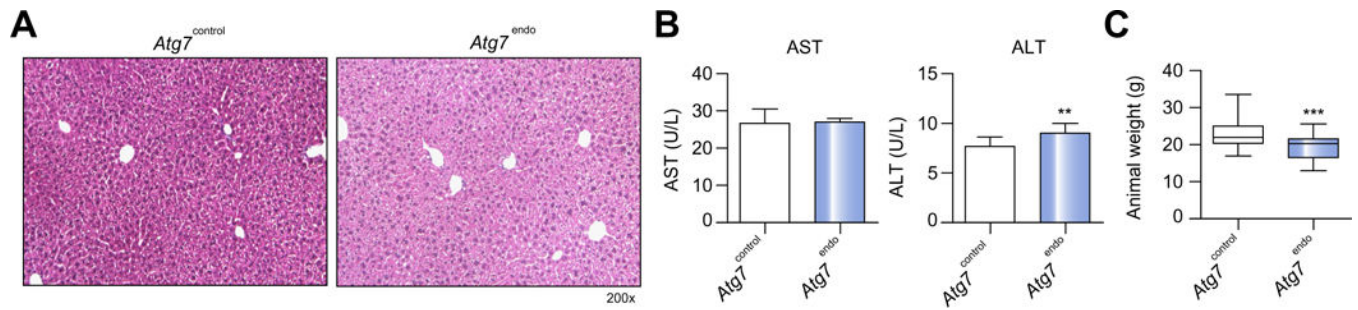


**Fig. 3. Loss of LSEC autophagy does not affect liver homeostasis.**

(A) Representative images of whole liver H&E staining showing a normal liver architecture. (B) Aminotransferase levels (n = 12) and (C) animal body weight (n = 69) from *Atg7*<sup>endo</sup> and *Atg7*<sup>control</sup> mice under basal conditions. Data shows mean value  $\pm$  SEM. (\**p* 0.05, \*\**p* 0.01, \*\*\**p* 0.001, Student's t test). H&E, hematoxylin and eosin; LSEC, liver sinusoid endothelial cell. (This figure appears in colour on the web.)

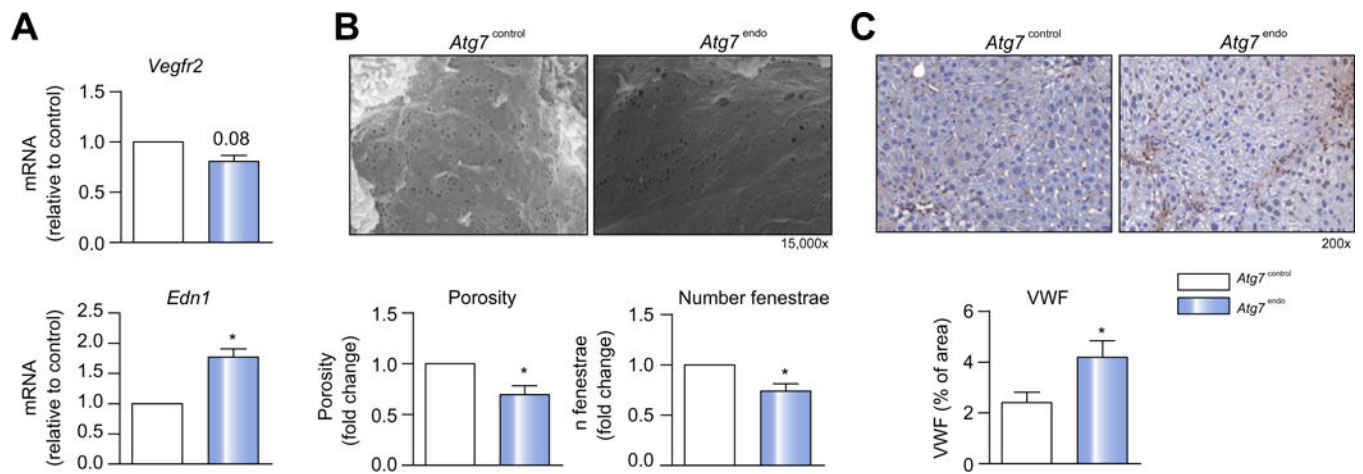


**Fig. 4. Loss of LSEC autophagy leads to cellular dysfunction.**

*Atg7<sup>endo</sup>* and *Atg7<sup>control</sup>* mice were treated every other day with CC1<sub>4</sub> i.p. for 1 week to induce mild acute liver injury. (A) mRNA changes (qPCR analysis) associated with endothelial dysfunction in primary isolated LSEC, showing a decrease in *Vegfr2* and an increase in *Edn1*. (B) SEM representative graphs of LSEC from *Atg7<sup>endo</sup>* and *Atg7<sup>control</sup>* mice with porosity and number of fenestrae quantification, showing a loss of fenestrae (capillarization) in the *Atg7<sup>endo</sup>* mice. (C) Whole liver sections stained for the endothelial dysfunction marker von Willebrand factor (vWF), displaying an increase value in *Atg7<sup>endo</sup>* mice. Data shows mean value  $\pm$  SEM (\**p* 0.05, \*\**p* 0.01, \*\*\**p* 0.001, Student's *t* test). LSEC, liver sinusoid endothelial cell; qPCR, quantitative real-time PCR. (This figure appears in colour on the web.)

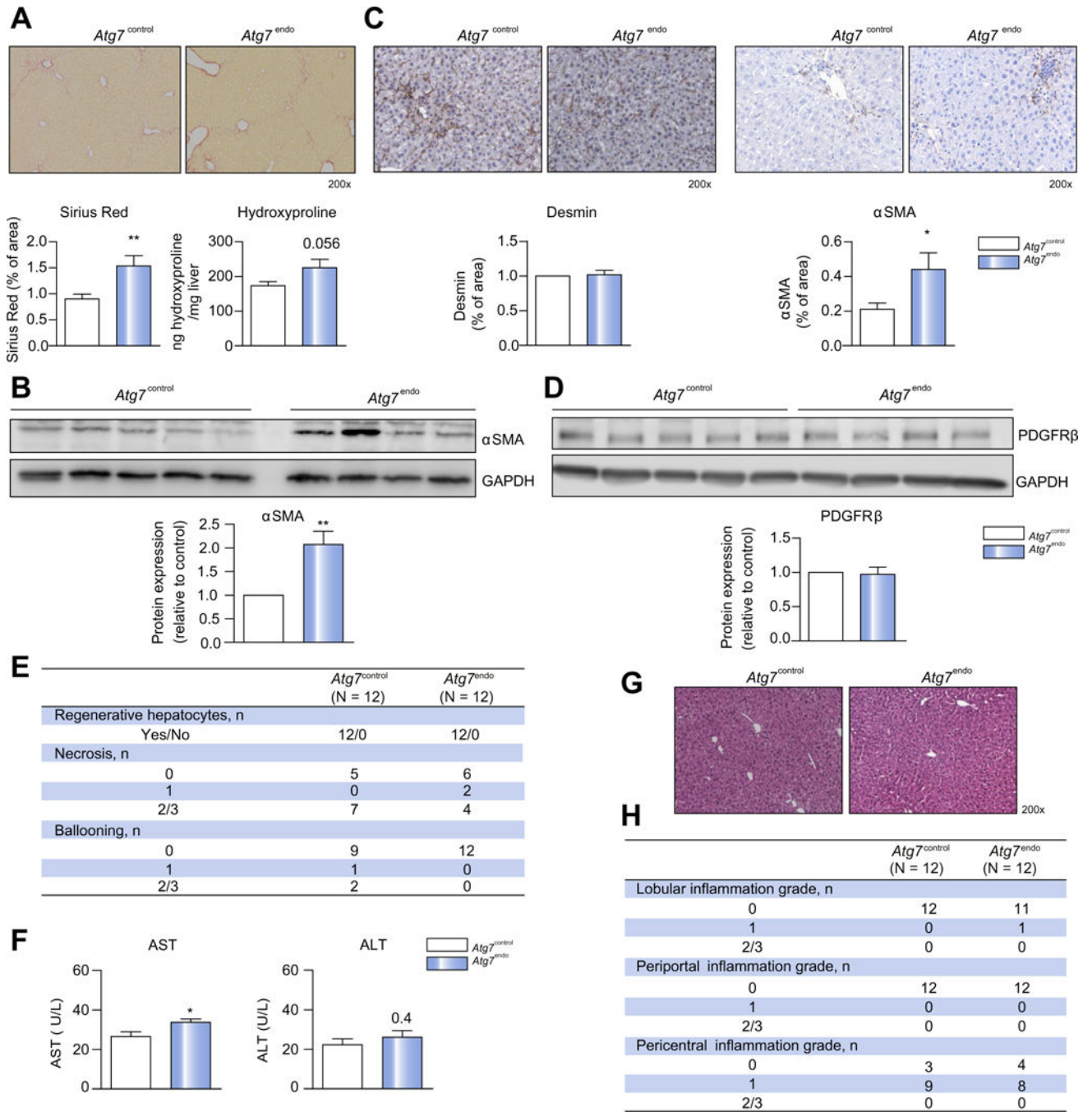


**Fig. 5. Loss of LSEC autophagy amplifies liver fibrosis without increasing liver injury.** *Atg7<sup>endo</sup>* and *Atg7<sup>control</sup>* mice were treated every other day with CC14 i. p. for 1 week to induce mild acute liver injury (n = 24). (A) Whole liver sections stained for Sirius Red and quantification of Sirius Red-positive area (left) and Hydroxyproline stain content (right). (B) Immunoblots for αSMA in isolated HSCs from *Atg7<sup>endo</sup>* and *Atg7<sup>control</sup>* mice and protein quantification. (C) Whole liver sections stained for desmin and αSMA and quantification of positive area. (D) Immunoblots for PDGFRB in whole liver from *Atg7<sup>endo</sup>* and *Atg7<sup>control</sup>* mice and protein quantification. (E) Histological liver analysis for hepatocyte regenerative

capacity and liver injury. (F) Aminotransferase levels showing an increase in aspartate aminotransferase with no change in alanine aminotransferase. (G) Representative images of whole liver sections stained for H&E and (H) histological liver analysis for inflammation scoring in *Atg<sup>endo</sup>* and *Atg<sup>control</sup>* mice after mild acute liver injury (CCl<sub>4</sub> i.p. for 1 week). Representative images are shown. Data shows mean value  $\pm$  SEM of at least 3 experiments (\**p* 0.05, \*\**p* 0.01, \*\*\**p* 0.001, Student's *t* test). CCl<sub>4</sub>, carbon tetrachloride; H&E, hematoxylin and eosin; HSC, hepatic stellate cell; LSEC, liver sinusoid endothelial cell.

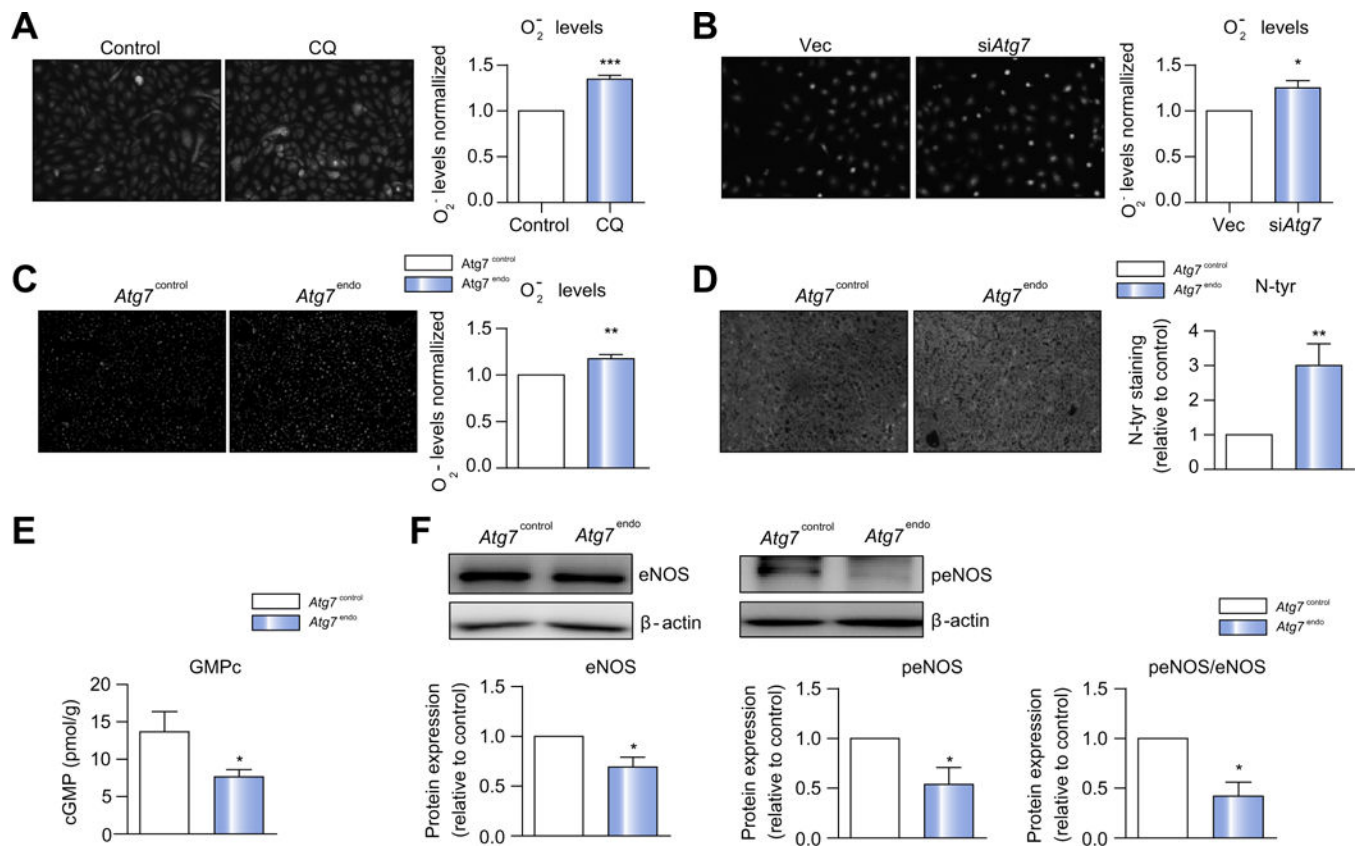


**Fig. 6. Loss of LSEC autophagy increases oxidative stress and decreases NO bioavailability.**

Cellular superoxide content measured by dihydroethidium in (A) HUVECs pre-treated with CQ for 12 h before  $H_2O_2$  was added for 15 h, (B) TSECs transduced with empty vector or siAtg7 were also treated with  $H_2O_2$  for 15 h and (C) in whole liver from  $Atg7^{endo}$  and  $Atg7^{control}$  mice after mild acute liver injury (CCl<sub>4</sub> i.p. for 1 week). (D) Quantitative nitrotyrosinated proteins analysis by fluorohistochemistry in whole liver tissue from  $Atg7^{endo}$  and  $Atg7^{control}$  mice after mild acute liver injury (CCl<sub>4</sub> i.p. for 1 week). (E) cGMP levels in liver homogenates from  $Atg7^{endo}$  and  $Atg7^{control}$  mice (CCl<sub>4</sub> i.p. for 1 week) illustrating a significant decrease. (F) Immunoblots for total eNOS and phosphorylated eNOS in whole liver from  $Atg7^{endo}$  and  $Atg7^{control}$  mice and protein quantification. Representative images are shown. Protein is expressed as fold-change relative to control. Data shows mean value  $\pm$  SEM of at least 3 experiments (\* $p$  0.05, \*\* $p$  0.01, \*\*\* $p$  0.001, Student's  $t$  test). CQ, chloroquine; HUVEC, human umbilical vein endothelial cell; LSEC, liver sinusoid endothelial cell; qPCR, quantitative real-time PCR; NO, nitric oxide; TSEC, mouse LSEC.

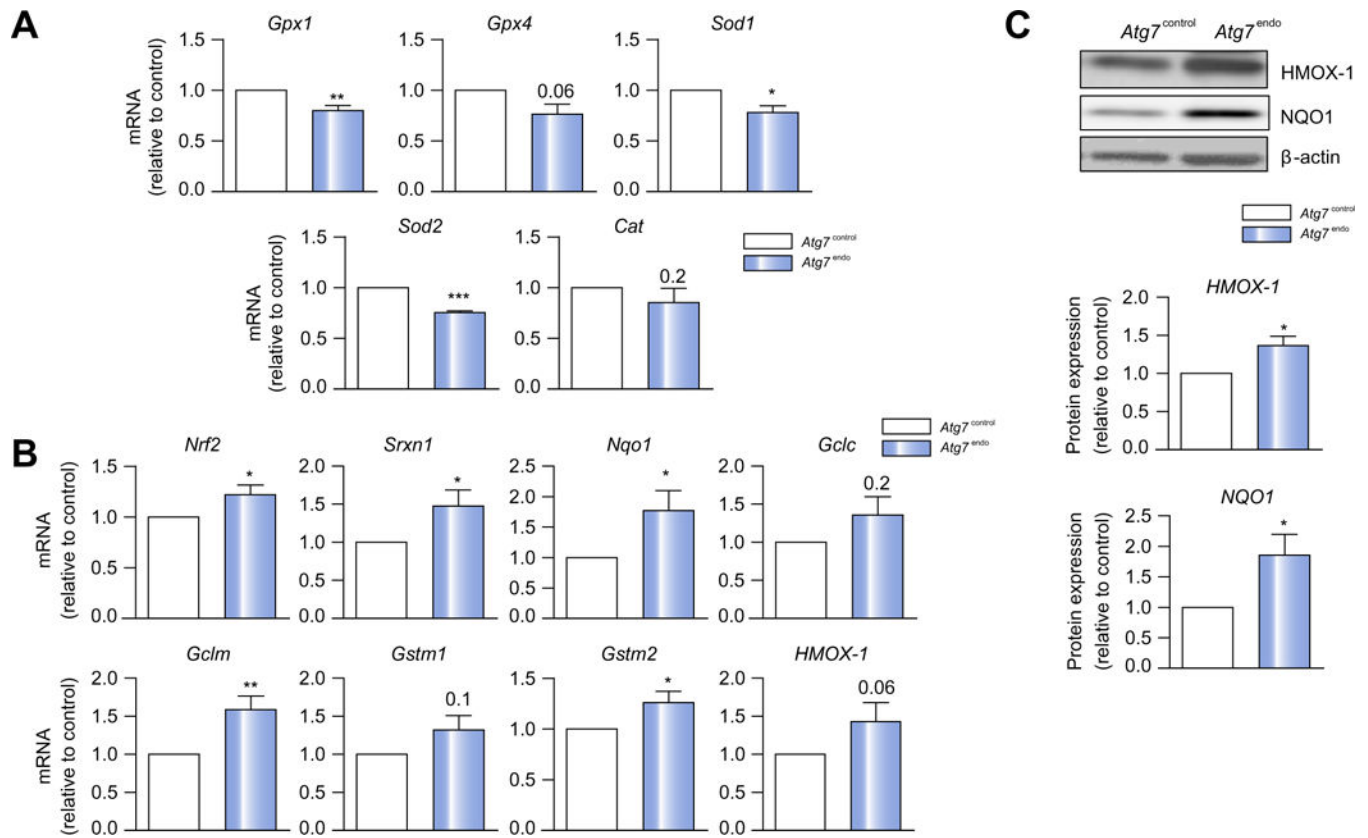


**Fig. 7. Loss of LSEC autophagy is associated with an insufficient antioxidant response.** *Atg7<sup>endo</sup>* and *Atg7<sup>control</sup>* mice were treated every other day with CCl<sub>4</sub> i. p. for 1 week to induce mild acute liver injury and primary LSECs were isolated. (A) mRNA changes (qPCR analysis) showing a downregulation of the classical genes that protect against oxidative stress *Gpx1*, *Gpx4*, *Sod1*, *Sod2* and *Cat* and (B) mRNA changes (qPCR analysis) showing upregulation of the Nrf2-dependent antioxidative stress genes *Srxn1*, *Nqo1*, *Gclc*, *Gclm*, and *Gstm2*. (C) Immunoblots for NQO1 and HMOX1 in isolated LSEC from *Atg7<sup>endo</sup>* and *Atg7<sup>control</sup>* mice confirming an increase at the protein levels. Data shows mean value  $\pm$  SEM of at least 3 experiments. mRNA expression is expressed as fold-change relative to control (\**p* 0.05, \*\**p* 0.01, \*\*\**p* 0.001, Student's *t* test). LSEC, liver sinusoid endothelial cell; qPCR, quantitative real-time PCR